nucleases.[10,11] The nucleophilic attack of a water oxygen on the vanadium nucleus of a lightly bound enzyme/nucleoside/vanadate complex accompanied by rearrangement in the ribonuclease active site to allow efficient hydrogen bonding of the histidine and serine nitrogens would lead directly to a pentacoordinate transition-state analogue of the normal phosphate intermediate. X-ray and neutron diffraction studies have revealed this structure in the uridine/vanadate/ribonuclease A complex.[12]

It is clear from this work that the −523 ppm signal is a composite signal corresponding to isomeric binuclear vanadium complexes as originally proposed[14-16] and this original assignment was not incorrect.[17-19] The proton NMR spectra support this conclusion and reveal that there are several types of nucleosides in the product complexes. Evidently from Figure 7, the major product (6.46 ppm) is symmetrical, since only one high-intensity (relative proportion 4.9) signal is observed. The same may be true for the second product (6.42 ppm) of relative intensity 1.4, but line broadening in the spectra indicates chemical exchange occurs in the second or so time scale. ^{1}H NMR spectroscopy may be able to provide further information concerning the equilibria established in this system. A close look at Figures 3-6 suggests there is a small degree of upward curvature in the experimental curves. It is possible that this is a result of the nonideal behavior of the ligands that was alluded to above. However, there is also the possibility that there is additional ligand incorporation into $V_2\ell_2$ to afford $V_2\ell_3$ or $V\ell_2$. If formed, these products should be observable in the proton spectra of high ligand concentration solutions even if the ligands do undergo base-stacking. The presence of significant proportions of $V\ell_2$ (or $V_2\ell_4$) at such high ligand concentrations might account for the discrepancy between the results presented here and the conclusions of other workers. Intensive investigation of these systems by 1- and 2-dimensional NMR techniques should resolve this question and provide detailed evidence concerning the structure of the products observed in this study.

Acknowledgment. Thanks are gratefully extended to the Medical Research Council of Canada (A.S.T., Grant MA-9470) and to the Deutsche Forschungsgemeinshaft (D.R., Grant Re 431/9-1) for their financial support of this work.

Registry No. Vanadate, 14333-18-7; inosine, 58-63-9; methyl β-D-ribofuranoside, 7473-45-2; adenosine, 58-61-7; guanosine, 118-00-3; uridine, 58-96-8; cytidine, 65-46-3; 2′-deoxyuridine, 951-78-0; 2′-deoxythymidine, 50-89-5.

Supplementary Material Available: Tables of reactant concentrations determined for the inosine/vanadate, adenosine/vanadate, uridine/vanadate, and cytidine/vanadate systems (7 pages). Ordering information is given on any current masthead page.

Contribution from the Département de Recherche Fondamentale/Service de Physique/SCPM and Laboratoires de Chimie/CC, 85 X, 38041 Grenoble Cedex, France, and Department of Molecular Biology, Research Institute of Scripps Clinic, La Jolla, California 92037

Magnetic Studies of the High-Potential Protein Model $[Fe_4S_4(S\text{-}2,4,6\text{-}(i\text{-}Pr)_3C_6H_2)_4]^-$ in the $[Fe_4S_4]^{3+}$ Oxidized State

J. Jordanov,*[1a,b] E. K. H. Roth,[1a] P. H. Fries,[1c] and L. Noodleman[1d]

Received February 5, 1990

The magnetic susceptibility of the title compound has been examined over the 5-320 K temperature range. The results have been analyzed by use of a spin-system Hamiltonian that includes two Heisenberg AF coupling parameters, $J_{12} = J + \Delta J_{12}$ and $J_{34} = J + \Delta J_{34}$, for the ferric ($\beta$) pair and the mixed-valence (α) pair, respectively, and one resonance delocalization parameter B for the α pair. The $[Fe_4S_4]^{3+}$ core follows the Curie-Weiss law $\chi_{mol} = 0.416/(T + 0.82)$ in the 5-15 K range. The 30-320 K range was well fitted with parameters $J = 571$ cm^{-1}, $B = 598$ cm^{-1}, and $\Delta J_{12} = 144$ cm^{-1} ($\Delta J_{34} = 0$), and $\langle g \rangle = 2.00$. The entire temperature range could be successfully fitted only by allowing the g values for the five lowest energy spin states to vary individually. Best fit parameters settled at $J = 652$ cm^{-1}, $B = 592$ cm^{-1}, and $\Delta J_{12} = 145$ cm^{-1}, and the two lowest lying energy levels $|^9/_2\ ^1/_2\ (4)\rangle$ and $|^7/_2\ ^1/_2\ (3)\rangle$ are nearly degenerate ($\Delta E = 11$ cm^{-1}). The coupling constants $J(Fe^{3+}\text{-}Fe^{3+}) = 797$ cm^{-1} and $J(Fe^{3+}\text{-}Fe^{2+}) = 652$ cm^{-1} are higher than those previously observed for Fe-Fe interactions in related clusters. Possible factors for this increase are the general compression of the $[Fe_4S_4]^{3+}$ core as compared with the $[Fe_4S_4]^{2+}$ core and also the distortion of the core. Further, fits involving both J and B parameters are conceptually distinctive from those using Heisenberg parameters alone.

Introduction

It is now well established that iron-sulfur proteins can exist under the three different redox states $[Fe_4S_4]^{1+}/[Fe_4S_4]^{2+}/[Fe_4S_4]^{3+}$, the first two core oxidation levels being used by ferredoxins, while the latter two are found in the so-called high-potential iron-sulfur proteins (HiPIP). The extensive studies by Holm and co-workers on the synthesis and characterization of the $[Fe_4S_4(SR)_4]^{3-/2-}$ model complexes[2] have given opportunity for detailed analysis of the cluster structural and electronic changes due to the electron transfer. In particular, it has been demonstrated that the reduced clusters[3] $[Fe_4S_4(SR)_4]^{3-}$ possess a more complex structural and ground-state variability than the one-electron-oxidized clusters $[Fe_4S_4(SR)_4]^{2-}$.

Similar studies of the highest core oxidation level have long been precluded by the observed instability[4] of the oxidized (either by chemical or electrochemical means) $[Fe_4S_4(SR)_4]^-$. Only recently, use of sterically encumbered thiolates has allowed for the stabilization[5] and isolation[6] of synthetic analogues with the $[Fe_4S_4]^{3+}$ core. The subsequent Mössbauer studies[7] have been done in the framework of an $S = {}^1/_2$ spin Hamiltonian, and the iron sites have been found to occur in two equivalent pairs. However, an appropriate spin-coupling model for oxidized Fe_4S_4 clusters has so far not been developed, in the sense that electron delocalization gives rise to substantial resonance interactions[8,9]

(1) (a) Service de Physique/SCPM. (b) Fédération de Biologie/PCV. (c) Laboratoires de Chimie/CC. (d) Scripps Clinic Research Institute.
(2) Berg, J. M.; Holm, R. H. In *Metal Ions in Biology*; Spiro, T. G., Ed.; Interscience: New York, 1982; Vol. 4, Chapter 1.
(3) (a) Carney, M. J.; Papaefthymiou, G. C.; Spartalian, K.; Frankel, R. B.; Holm, R. H. *J. Am. Chem. Soc.* **1988**, *110*, 6084. (b) Carney, M. J.; Papaefthymiou, G. C.; Whitener, M. A.; Spartalian, K.; Frankel, R. B.; Holm, R. H. *Inorg. Chem.* **1988**, *27*, 346. (c) Carney, M. J.; Papefthymiou, G. C.; Frankel, R. B.; Holm, R. H. *Ibid.* **1989**, *28*, 1497.
(4) (a) de Pamphilis, B. V.; Averill, B. A.; Herskovitz, T.; Que, L., Jr.; Holm, R. H. *J. Am. Chem. Soc.* **1974**, *96*, 4159. (b) Mascharak, P. K.; Hagen, K. S.; Spence, J. T.; Holm, R. H. *Inorg. Chim. Acta* **1983**, *80*, 157. (c) Christou, G.; Garner, C. D.; Drew, M. G. B.; Cammack, R. J. *J. Chem. Soc., Dalton Trans.* **1981**, 1550.
(5) Ueyama, N.; Terakawa, T.; Sugawara, T.; Fuji, M.; Nakamura, A. *Chem. Lett.* **1984**, 1287.
(6) O'Sullivan, T.; Millar, M. M. *J. Am. Chem. Soc.* **1985**, *107*, 4096.
(7) Papaefthymiou, V.; Millar, M. M.; Münck, E. *Inorg. Chem.* **1986**, *25*, 3010.

0020-1669/90/1329-4288$02.50/0

Table I. Magnetic Properties of $[Et_4N][Fe_4S_4(S\text{-}2,4,6\text{-}(i\text{-}Pr)_3C_6H_2)_4]$

C, emu K/G	Θ, K	T range, K[a]	J, cm^{-1} [b]	B, cm^{-1} [b]	ΔJ_{12}, cm^{-1} [b]
0.416	−0.82	5–15	652	592	145

[a] Curie–Weiss region. [b] Parameters obtained from best least-squares fitting (see fit V in Table II).

and that, therefore, the usual Heisenberg Hamiltonian is not suitable for the description of such systems.

Recently, one of us has proposed a theoretical model for the spin states of the oxidized $[Fe_4S_4]^{3+}$ clusters.[10] It was of interest to test the validity of this model through the predicted energy level scheme by techniques such as magnetic susceptibility. In this paper, we report the magnetic susceptibility data of $[Et_4N][Fe_4S_4(S\text{-}2,4,6\text{-}(i\text{-}Pr)_3C_6H_2)_4]$ and the results of their fit with this new model.

Experimental Section

Preparation of Sample. $(Et_4N)[Fe_4S_4(S\text{-}2,4,6\text{-}(i\text{-}Pr)_3C_6H_2)_4]$ (**1**) was prepared under argon by controlled-potential electrolysis at +0.5 V of 275 mg of $(Et_4N)_2[Fe_4S_4(S\text{-}2,4,6\text{-}(i\text{-}Pr)_3C_6H_2)_4]$ in 35 mL of dichloromethane, followed by evaporation to dryness. The final solid contained 21.3% of compound **1** and 78.7% of electrolyte Bu_4NPF_6. Finely ground samples of 40–100 mg were prepared for magnetic measurements, and frozen CH_2Cl_2 solutions were used for EPR spectroscopy.

Physical Measurements. Magnetic data were obtained by use of an SHE Corp. SQUID susceptometer. Magnetization measurements were carried out at 5 K and at applied fields varying between 1 and 15 kOe.

Magnetic susceptibility data were measured at 2.5 kOe and in the 5–320 K temperature range. Several samples from different preparations were used and gave reproducible results to ±1%. Sample holder and electrolyte magnetizations were subtracted from the raw data, and the molar susceptibilities were also corrected for ligand diamagnetism.[11]

EPR spectra were recorded at X-band frequency and 4–30 K on a Varian E 109 instrument equipped with an Oxford Instruments ESR 900 cryostat, an EIP 548 A frequency counter, and a Varian NMR gaussmeter.

Electrochemistry was performed with a PAR 273 potentiostat and by use of a four-electrode system allowing simultaneous electrolysis and cyclic voltammetry. Working and counter electrodes were of platinum; the reference Ag/Ag^+ electrode was a silver wire immersed in a AgI-saturated CH_2Cl_2 solution containing the supporting electrolytes Bu_4NPF_6 (0.1 M) and Bu_4NI (0.02 M).

Results and Discussion

The oxidized cluster $[Et_4N][Fe_4S_4(S\text{-}2,4,6\text{-}(i\text{-}Pr)_3C_6H_2)_4]$ was prepared by controlled-potential electrolysis (instead of chemical oxidation by $[(C_5H_5)_2Fe]BF_4$ as previously published), and the cluster concentration was checked by spin integration of the EPR signal at $g = 2.06$ (4.2 K). It was thus obtained in a very pure form (the impurity at $g = 1.960$ sometimes present after chemical oxidation was absent, and no low-field resonances were observed) and also at a 5-fold dilution by the electrolyte, which should produce a decrease of intercluster spin–spin interactions. Magnetization measurements at $T = 5$ K and at fields varying between 1 and 15 kOe are linear up to 3 kOe. Magnetic susceptibility data were therefore recorded at the limiting field 2.5 kOe and as a function of temperature, between 5 and 320 K.

The results are plotted in Figure 1, and selected constants are listed in Table I. At low temperatures (5–15 K), the cluster obeys the Curie–Weiss relation (eq 1) with a very small Weiss constant

$$\chi_{mol} = C/(T - \Theta) \quad (1)$$

Θ. The Curie constant is in good agreement with the theoretical value for $S_{tot} = {}^1/_2$ (0.375 emu K/G). Above the Curie range, a negative deviation from linear behavior is observed for $1/\chi_{mol}$ vs T. This is consistent with the occupancy of thermally populated

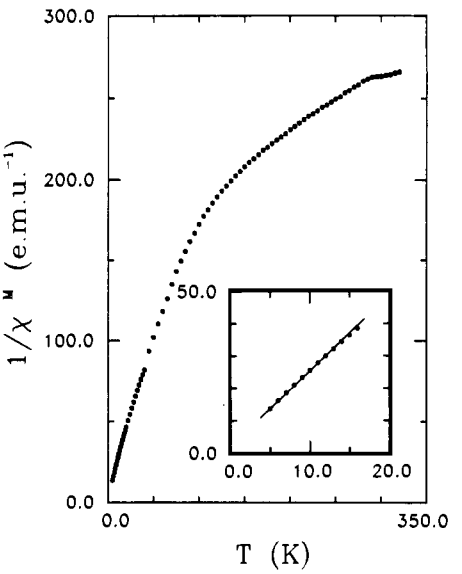

Figure 1. Temperature dependence of the reciprocal molar susceptibility for $(Et_4N)[Fe_4S_4(S\text{-}2,4,6\text{-}(i\text{-}Pr)_3C_6H_2)]$. The solid line through the data is a least-squares fitting of the Curie–Weiss region. The insert is an expansion of the 5–15 K range.

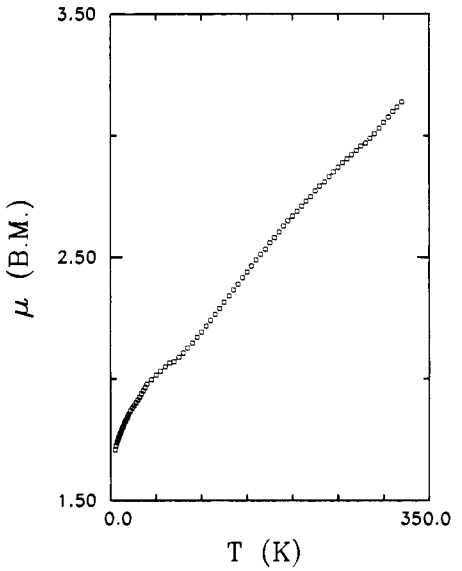

Figure 2. Plot of effective magnetic moment per $(Et_4N)[Fe_4S_4(S\text{-}2,4,6\text{-}(i\text{-}Pr)_3C_6H_2)_4]$ molecule versus temperature.

excited states with total spin $S > {}^1/_2$, arising from antiferromagnetic coupling, as also shown by the increasing effective magnetic moment with increasing temperatures (see Figure 2).

We have analyzed the whole range data[12] with the following system spin Hamiltonian:

$$H = J(\vec{S}_1\cdot\vec{S}_2 + \vec{S}_1\cdot\vec{S}_3 + \vec{S}_1\cdot\vec{S}_4 + \vec{S}_2\cdot\vec{S}_3 + \vec{S}_2\cdot\vec{S}_4 + \vec{S}_3\cdot\vec{S}_4) \pm B(S'_{34} + {}^1/_2) + \Delta J_{12}(\vec{S}_1\cdot\vec{S}_2) + \Delta J_{34}(\vec{S}_3\cdot\vec{S}_4) \quad (2)$$

(8) (a) Noodleman, L.; Baerends, E. J. *J. Am. Chem. Soc.* **1984**, *106*, 2316. (b) Aizman, A.; Case, D. A. *Ibid.* **1982**, *104*, 3269. (c) Noodleman, L.; Norman, J. G., Jr.; Osborne, J. H.; Aizman, A.; Case, D. A. *Ibid.* **1985**, *107*, 3418.

(9) (a) Belinskii, M. I.; Tsukerblat, B. S.; Gerbeleu, N. V. *Sov. Phys.—Solid State (Engl. Transl.)* **1983**, *26*, 1142. (b) Girerd, J. J. *J. Chem. Phys.* **1983**, *79*, 1766.

(10) Noodleman, L. *Inorg. Chem.* **1988**, *27*, 3677.

(11) O'Connor, C. J. *Prog. Inorg. Chem.* **1982**, *29*, 203.

(12) For comparison purposes, we have also fitted the data with a pure Heisenberg model and, upon suggestion by a reviewer, we report here the results. Since the eigenstates are highly degenerate in the absence of the B term, we have included all 27 microstates due to $S = {}^1/_2$ (10 states) and to $S = {}^3/_2$ (17 states), as obtained from ref 10. When the 5–320 K data are evaluated by constraining g to 2.00 and with $\Delta J_{12} \neq 0$, a rather poor fit is obtained ($\sqrt{R} = 17.8 \times 10^{-3}$), with $J = 899$ cm^{-1} and $\Delta J_{12} = 73$ cm^{-1}. Twelve distinct energies are then observed for the 27 states. When ΔJ_{12} is set to 0, J stays unchanged, and only two distinct energies remain, one for $S = {}^1/_2$ and one for $S = {}^3/_2$. When g is constrained to a value higher than 2.00 ($g = 2.05$), this does not improve the quality of the fit, but J settles at 388 cm^{-1}, a more reasonable value. On the other hand, the higher temperature range (30–320 K) can be accurately fitted ($\sqrt{R} = 15.4 \times 10^{-5}$) with the parameters settling at $g = 2.00$, $J = 397$ cm^{-1}, and $\Delta J = 0$. The Heisenberg-only model lowers the J value and tends not to discriminate among the coupling constants of the various Fe–Fe interactions within the cluster.

Table II. Parameters Obtained from the Least-Squares Fitting of the Magnetic Susceptibility Data

param	fit I[b]	fit II[b]	fit III[b]	fit IV[c]	fit V[c]
T range, K	5–320	30–320	30–320	30–320	5–320
no. of magnetic states	27	27	5	27	5
J, cm^{-1}	859	542	571	570	652
B, cm^{-1}	39	553	598	603	592
ΔJ_{12}, cm^{-1}	194	134	144	144	145
B/J	0.045	1.02	1.04	1.05	0.9
$\Delta J_{12}/J$	0.22	0.24	0.25	0.25	0.22
$\langle g \rangle$	2.00	2.00	2.00	1.92	1.90, 2.20, 1.90, 1.92, 1.97
$\sqrt{R}$[a]	45×10^{-5}	7.7×10^{-5}	7.4×10^{-5}	6.8×10^{-5}	13.4×10^{-5}

[a] Goodness of fit. [b] $\langle g \rangle$ kept fixed. [c] $\langle g \rangle$ allowed to vary.

where the Fe site spins are $S_1 = S_2 = S_3 = {}^5/_2$ and $S_4 = 2$ and the Fe atoms are involved in two different pairs

β pair

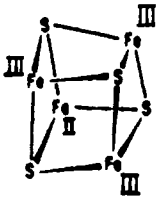

α pair

the mixed-valence α pair and the ferric β pair. J is the interlayer coupling constant linking one site of pair α with one site of pair β, while the β and α pair couplings are $J_{12} = J + \Delta J_{12}$ and $J_{34} = J + \Delta J_{34}$, respectively. The simpler, but still physically significant, case includes $\Delta J_{12} > 0$ and $\Delta J_{34} = 0$. B is the resonance delocalization term that accounts for the spin parallel alignment within the α pair. This term was first introduced in another system by Anderson and Hasegawa[13] and in iron–sulfur clusters by Papaefthymiou et al.[13] to model the $[Fe_3S_4]^0$ spin states and by Noodleman[10] to model the $[Fe_4S_4]^{3+}$ spin states. The general solution to eq 2 with $\Delta J_{34} = 0$ is then

$$E(S'_{34}, S, S'_{12}) = (J/2)[S(S+1)] - B(S'_{34} + {}^1/_2) + \Delta J_{12}[S'_{12}(S'_{12}+1)] \quad (3)$$

where S'_{34} and S'_{12} are the spin values of the mixed-valence α pair and of the ferric β pair, respectively, and where S is the total spin. The general expression of the theoretical molar magnetic susceptibility $\chi_{th}(T)$ for a powder or a frozen solution is obtained as a sum over all the multiplets $|S'_{34}, S, S'_{12}\rangle$:

$$\chi_{th}(T) = \frac{N\mu_B{}^2}{3k_BT} \times \frac{\sum_{|S'_{34},S,S'_{12}\rangle} [g(S'_{34}, S, S'_{12})]^2 S(S+1)(2S+1) e^{-\beta E(S'_{34},S,S'_{12})}}{\sum_{|S'_{34},S,S'_{12}\rangle} (2S+1) e^{-\beta E(S'_{34},S,S'_{12})}} \quad (4)$$

where $\beta = 1/k_BT$ and where the factors $g(S'_{34}, S, S'_{12})$ depend on the multiplet. In eqs 2 and 3, the exchange constants J and ΔJ_{12} and resonance term B are unknown parameters that can be determined through a least-square fit of the susceptibility data $\chi_{ex}(T)$ as a function of the temperature T. More precisely, denoting by T_i ($i = 1-n_T$) the different temperatures of the susceptibility measurements, our aim is to minimize the normalized residual:[14]

$$R = \frac{1}{n_T} \sum_{i=1}^{n_T} [\chi_{ex}(T_i) - \chi_{th}(T_i)]^2 \quad (5)$$

To a first approximation, if we assume that the g factors of the various magnetic ions are isotropic, with values g_{ion} close the free electron value, it is possible to calculate the factors $g(S'_{34}, S, S'_{12})$ of the multiplets from the above Hamiltonian model (2) as a function of the unknown g_{ion}. The factors $g(S'_{34}, S, S'_{12})$ corresponding to the lowest energy levels are near one another and are thus considered as identical, when they are fitted in least-squares refinements I–IV. This simplification is then removed in further attempts (fit V). Finally, the presence of a monomeric magnetic impurity of unknown concentration and g factor is also taken into account in the fitting procedure, together with the correlated inaccuracy of the weight of the iron cluster.

Scheme I

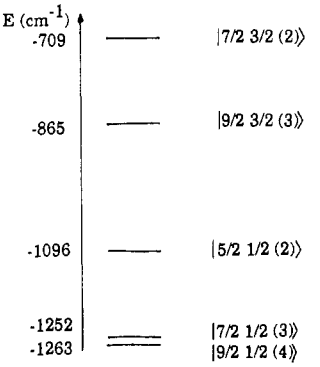

Table II lists the values of J, B, ΔJ_{12}, g, and $\sqrt{R}$ obtained from the various least-squares refinements,[14] and Table S1 lists the observed values of χ_{mol} as a function of temperature.[15]

In the first time, the experimental data were evaluated over the whole temperature range (5–320 K) and by constraining the average g value to 2.00, as obtained from the EPR measurement of the solid.[7] This gave a rather poor fit ($\sqrt{R} = 45 \times 10^{-5}$; see fit I in Table II) and unreasonable parameters ($J = 859$ cm^{-1} and $B/J = 0.045$). A considerably better agreement was obtained when the experimental data below 30 K were not taken into consideration (fit II). The refinements also produce an ordering in energy of the 27 magnetic states that are in principle available to the system. It was noticed, however, that when the relevant magnetic states are limited to the ground state and the four lowest excited states, the quality of refinement remains essentially unchanged (fit III), with small increases in J from 542 to 571 cm^{-1} and B from 553 to 598 cm^{-1}. The effect of the variation of g from a value of 2.00 was also tested. An equally good agreement was obtained with $g = 1.92$ (see fit IV), over all of the 27 magnetic states.

Finally, a least-squares fitting of eq 4 to the data over the entire temperature range was performed by taking into consideration the five lowest lying spin states and by considering the corresponding g_1, g_2, g_3, g_4, and g_5 as variable parameters. The results for this last refinement are shown in Table II (fit V), and the theoretical fit using these parameters is shown in Figure 3. When

(13) (a) Anderson, P. W.; Hasegawa, H. *Phys. Rev.* **1955**, *100*, 675. (b) Papaefthymiou, V.; Girerd, J. J.; Moura, I.; Moura, J. J. G.; Münck, E. *J. Am. Chem. Soc.* **1987**, *109*, 4703. Münck, E.; Papafthymiou, V.; Surerus, K. K.; Girerd, J. J. In *Metals in Proteins*; Que, L., Ed.; ACS Symposium Series: American Chemical Society: Washington, DC, 1988.

(14) Gill, P. E.; Murray, W.; Wright, M. H. *Practical Optimization*; Academic Press: New York, 1981. The minimization is performed by use of a combination of the polytope or simplex algorithm and a quasi-Newton method implemented in the 1976 version of program MINUIT at the CERN computer center library.

(15) See supplementary material.

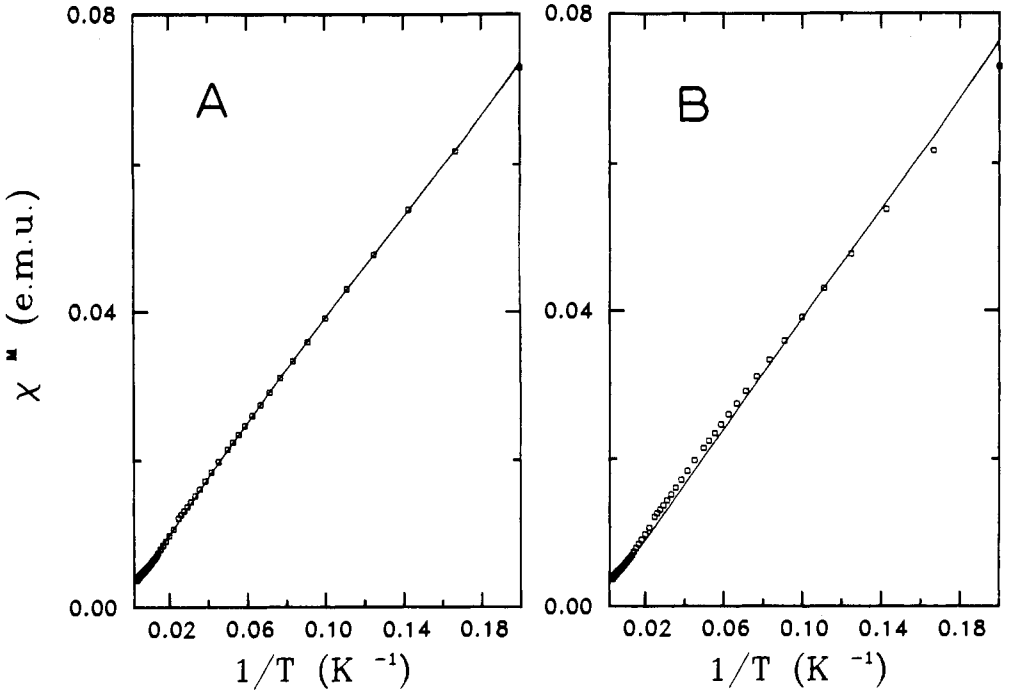

Figure 3. Molar susceptibility versus reciprocal temperature for $(Et_4N)[Fe_4S_4(S\text{-}2,4,6\text{-}(i\text{-}Pr)_3C_6H_2)_4]$. Experimental data are shown as open squares. (A) shows the theoretical fit to all the experimental data, using the parameters of fit V in Table II. (B) shows the theoretical fit to all the experimental data, using the best fit parameters (fit II) of the high-temperature range, for comparison purposes.

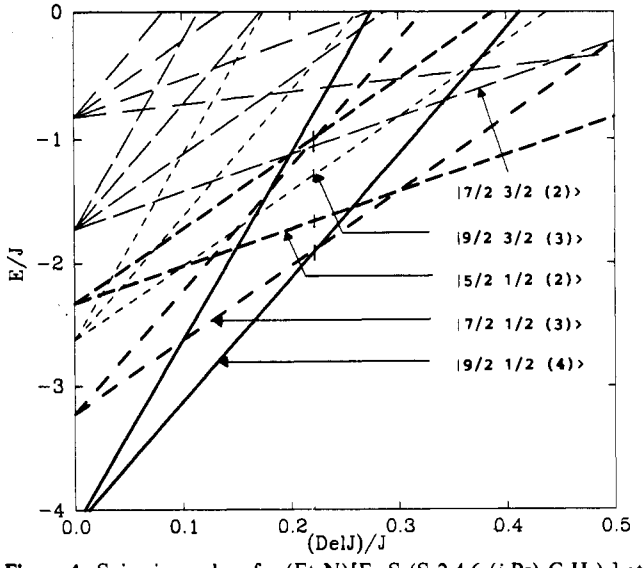

Figure 4. Spin eigenvalues for $(Et_4N)[Fe_4S_4(S\text{-}2,4,6\text{-}(i\text{-}Pr)_3C_6H_2)_4]$ at $B/J = 0.9$.

compared to the previous fit including *all* the experimental data (fit I), the agreement factor of fit V has considerably improved. Parameters B and J have slightly increased, to 592 and 652 cm^{-1}, respectively, whereas B/J remains approximately constant at 0.9 and $\Delta J_{12}/J$ is somewhat smaller at 0.22. In Figure 4, we have plotted the low-lying eigenstates $|S'_{34}\, S\, (S'_{12})\rangle$ at $B/J = 0.9$ and $\Delta J_{12}/J = 0.22$ as in fit V. Scheme I shows the ground state and the first four excited states with their relative energies.

These results call for several comments. In a first step, when only the higher temperature ($T \geq 30$ K) data were fitted, it appeared that considering either the 27 available spin states, or only the 5 lowest, made little difference. This suggests that there is very little contribution to the magnetic susceptibility from any spin states with higher energies. Also, when all the states were taken into consideration and $\langle g \rangle$ was allowed to vary, the agreement improved by reducing the value of $\langle g \rangle$ to 1.92. This observation motivated us to try to fit the susceptibility data using the five lowest energy spin states, obtained from the Hamiltonian of eq 2 as before, and allowing five individual g's as variable parameters, this time over the entire range of T, from 5 to 320 K. A much better fit was obtained (fit V) than previously (fit I), and the g values for the five lowest lying spin states settled at $g_1 = 1.90$, $g_2 = 2.20$, $g_3 = 1.90$, $g_4 = 1.92$, and $g_5 = 1.97$. The first three levels average to $\langle g \rangle = 2$, but the variability in g from state to state is larger than that displayed in the low-temperature EPR spectrum of the polycrystalline material. There may be an association between the increasing magnetic moment observed at low temperature (Figure 2) and the broad EPR spectrum observed at $T = 9.2$ K.[7] This increase in effective magnetic moment at low temperature is possibly related to a decrease of cluster–cluster interactions. While the dilution in electrolyte would diminish such effects, they appear to be present still. Also, the two states $|^9/_2\ ^1/_2\ (4)\rangle$ and $|^7/_2\ ^1/_2\ (3)\rangle$ appear from the modeling to be nearly degenerate and may well have sufficiently different electronic structure to possess different g(av) values. Further, there may be a distribution of cluster conformations ("g strain"[16,17]) and of α and β pairs over the Fe sites, which would give such a distribution of g values. We therefore rely on fit V to give us the most dependable B and J parameters, as it includes the entire temperature range (5–320 K) where, in particular, the Curie–Weiss relation is obeyed. Close attention should also be paid to fits II and III as they give an accurate fit to the higher (30–320 K) temperature range and include fewer parameters.

Energy level Scheme I shows the pattern of the low-lying energy levels. There is a near degeneracy between the $S = {}^1/_2$ states $|S'_{34}\ S\ (S'_{12})\rangle = |^9/_2\ ^1/_2\ (4)\rangle$ and $|^7/_2\ ^1/_2\ (3)\rangle$, the separation being only 11 cm^{-1}, with $|^5/_2\ ^1/_2\ (2)\rangle$ higher by about 167 cm^{-1}; the first $S = {}^3/_2$ state $|^9/_2\ ^3/_2\ (3)\rangle$ is about 398 cm^{-1} above the ground state and $|^7/_2\ ^3/_2\ (2)\rangle$ is at 554 cm^{-1}. Fit III gives the position of the first two excited $S = {}^3/_2$ states at 282 and 449 cm^{-1} above the $S = {}^1/_2$ ground state. This relative spin-state ordering for the first five states is the same as in fit V, and the energy differences among the first three $S = {}^1/_2$ states (ground plus two excited states) are very close to that obtained from fit V. The predicted B/J ratio is 0.9 and $\Delta J_{12}/J = 0.22$ from fit V. This

(16) Orme-Johnson, W. H.; Sands, R. H. In *Iron-Sulfur Proteins*; Lovenberg, W., Ed.; Academic Press: New York, 1973; Vol. 2, Chapter 5.
(17) (a) Hagen, W. R.; Hearshen, D. O.; Sands, R. H.; Dunham, W. R. *J. Magn. Reson.* **1985**, *61*, 220. (b) Hagen, W. R.; Hearshen, D. O.; Harding, L. J.; Dunham, W. R. *Ibid.* **1985**, *61*, 233. (c) More, C.; Bertrand, P; Gayda, J. P. *Ibid.* **1987**, *73*, 13.

B/J is somewhat smaller than the range predicted in our previous paper, $B/J > 1.4$,[10] and the interlayer coupling constant $J = 652$ cm^{-1} is higher than predicted on theoretical grounds ($J = \sim 390$ cm^{-1} and $B/J = \sim 1.5$ from recent Xα SW calculations[18]). It is larger than is typical of experimental results from comparable clusters as will be discussed in more detail below. The ratio $\Delta J_{12}/J = 0.22$ is very similar to that found theoretically from comparing oxidized and reduced forms of $[Fe_3S_4]^{+/0}$ clusters.[19] Fit V gives $J_{12} = J + \Delta J_{12} = 797$ cm^{-1} for the ferric pair coupling constant; the mixed-valence pair coupling $J_{34} = J = 652$ cm^{-1}, since by assumption ΔJ_{34} was set equal to 0. The ferric pair coupling is the easiest to compare with previous measurements in oxidized Fe_2S_2 and Fe_3S_4 systems, since in these systems there is no resonance delocalization (no B terms) of mixed-valence sites to complicate the analysis. J_{12} is higher than found experimentally for oxidized sites in $[Fe_2S_2(S_2\text{-}o\text{-xyl})_2]^{2-}$ (300 cm^{-1})[20] and $[Fe_2S_2Cl_4]^{2-}$ (316 cm^{-1})[21] and in oxidized 2 Fe ferredoxins (ca. 370 cm^{-1})[22] and the oxidized linear Fe_3S_4 cluster $[Fe_3S_4(SEt)_4]^{3-}$ ($\geq$300 cm^{-1}).[23]

For the oxidized Fe_4S_4 cluster in *C. vinosum* HiPIP,[24] the measured Heisenberg coupling constant was 200 cm^{-1}, which may be compared to an average J over all pairs of 676 cm^{-1} from fit V ($J_{av} = (4J + J_{34} + J_{12})/6$). This measurement,[24] however, is subject to caution, as it was performed by use of an analytical balance magnetometer, which probably gives less reliable experimental data than a superconducting quantum magnetometer (SQUID).[25] Further, the analysis of data by a Heisenberg model alone is not reliable in the presence of a delocalized mixed-valence pair, so that a direct comparison of "experimental" J parameters from this model with that of a J, B model is really a comparison between rather different physical quantities. As a further relevant experimental system, we cite the fitting of the magnetic susceptibility of $[Fe_4S_4(SPh)_4]^{2-}$ again by a Heisenberg Hamiltonian,[26] where $J(Fe^{2+}\text{–}Fe^{3+}) = 500$ cm^{-1}, $J(Fe^{3+}\text{–}Fe^{3+}) = 550$ cm^{-1}, and $J(Fe^{2+}\text{=}Fe^{2+}) = 450$ cm^{-1}. These values are smaller than those we find from fit V to the $[Fe_4S_4]^{3+}$ cluster, but they are much closer to our fit than that for *C. vinosum* HiPIP. Day et al.[25] have previously established that the accuracy of magnetization measurements generally improves with a higher spin concentration in the sample, so that more accurate measurements can be made on synthetic clusters than on metalloproteins. This advantage occurs at the cost of enhanced cluster–cluster interactions.

Examining possible factors leading to higher J parameters than in comparable systems,[27] we note a general compression of the $[Fe_4S_4]^{3+}$ core compared with the synthetic $[Fe_4S_4]^{2+}$ oxidation state, average Fe–S and Fe–SR bonds being shorter by about 0.02 and 0.04 Å.[6,28] Further, $[Fe_4S_4]^{3+}$ are distorted cubanes, with the Fe–Fe distances spanning up to 0.03 Å in the synthetic cluster considered here (2.724, 2.728, 2.749, 2.754 Å).[29]

In summary, using a combined Heisenberg plus resonance coupling Hamiltonian, we have been able to fit the magnetic susceptibility data accurately from 30 to 320 K with only three variable parameters, J, J_{12}, and B. The g(av) value was fixed at 2.0 as determined from experimental EPR studies at low T. The low-temperature data *as well as* the high-temperature data can be fitted only by allowing different g values for the five lowest spin states. Those may indeed have sufficiently different electronic structures to possess different g(av) values, but a proper physical model for the low-temperature magnetic data remains elusive. The J parameters derived from the fits are larger than those usually observed for Fe–Fe interactions in related clusters and oxidation states. Part of this discrepancy may be due to a small contraction of the FeS core compared to the 2+ oxidation level. Fits involving both J and B parameters are conceptually distinctive from those using Heisenberg parameters only.[12] There is a need for accurate susceptibility measurements on delocalized mixed-valence clusters and fitting procedures where resonance delocalization is included. With such an approach, a reasonable data base can be constructed including both J and B parameters in a variety of systems. Since susceptibility is sensitive only to the total spin quantum numbers of the states, their relative energies, and their respective g values, it is highly desirable to complement such measurements with EPR observations and other spectroscopic data (Mössbauer, ENDOR, optical) to gain a better understanding of the detailed spin coupling of the system.

Acknowledgment. We thank Drs. B. Lamotte and J. Gaillard for useful discussions. L.N. thanks the National Institutes of Health (Grant GM 39914) for financial support.

Registry No. $[Fe_4S_4(S\text{-}2,4,6\text{-}(i\text{-}Pr)_3C_6H_2)_4]^-$, 96455-60-6.

Supplementary Material Available: Table S1, giving the observed values of χ_{mol} as a function of temperature (1 page). Ordering information is given on any current masthead page.

(18) Noodleman, L. Unpublished work.
(19) Sontum, S. F.; Noodleman, L.; Case, D. A. In *Computational Chemistry: The Challenge of d and f Electrons*; Salahub, D. R., Zerner, M., Eds.; ACS Symposium Series; American Chemical Society: Washington, DC, 1989.
(20) Gillum, W. O.; Frankel, R. B.; Foner, S.; Holm, R. H. *Inorg. Chem.* **1976**, *15*, 1095.
(21) Wong, G. B.; Bobrik, M. A.; Holm, R. H. *Inorg. Chem.* **1978**, *17*, 578.
(22) (a) Palmer, G.; Dunham, W. R.; Fee, J. A.; Sands, R. H.; Iizuka, T.; Yonetani, T. *Biochim. Biophys. Acta* **1971**, *245*, 201. (b) Petersson, L.; Cammack, R.; Rao, K. K. *Biochim. Biophys. Acta* **1980**, *622*, 18.
(23) Girerd, J. J.; Papaefthymiou, G. C.; Watson, A. D.; Gamp, E.; Hagen, K. S.; Edelstein, N.; Frankel, R. B.; Holm, R. H. *J. Am. Chem. Soc.* **1984**, *106*, 5941.
(24) Antanaitis, B. C.; Moss, T. H. *Biochim. Biophys. Acta* **1975**, *405*, 262.
(25) Day, E. P.; Kent, T. A.; Lindahl, P. A.; Münck, E.; Orme-Johnson, W. H.; Roder, H.; Roy, A. *Biophys. J.* **1987**, *52*, 837.
(26) Papaefthymiou, G. C.; Laskowski, E. J.; Frota-Pessoa, S.; Frankel, R. B.; Holm, R. H. *Inorg. Chem.* **1982**, *21*, 1723.
(27) Noodleman, L.; Case, D. A.; Aizman, A. J. *J. Am. Chem. Soc.* **1988**, *110*, 1001.
(28) (a) Hagen, K. S.; Watson, A. D.; Holm, R. H. *Inorg. Chem.* **1984**, *23*, 2984. (b) Stephan, D. W.; Papaefthymiou, G. C.; Frankel, R. B.; Holm, R. H. *Inorg. Chem.* **1983**, *22*, 1558.
(29) As only selected distances have been published for this cluster,[5] we have recalculated the Fe–Fe distances from the fractional atomic coordinates available as supplementary material from ref 6.